# An Algorithm for Wireless Relay Placement

Jillian Cannons, *Member, IEEE,* Laurence B. Milstein, *Fellow, IEEE,* and Kenneth Zeger, *Fellow, IEEE*

***Abstract*—An algorithm is given for placing relays at spatial positions to improve the reliability of communicated data in a sensor network. The network consists of many power-limited sensors, a small set of relays, and a receiver. For each sensor, the receiver receives a direct signal as well as an indirect signal from one of the available relays. The relays rebroadcast the transmissions in order to achieve diversity at the receiver. Both amplify-and-forward and decode-and-forward relay networks are considered. Channels are modeled with Rayleigh fading, path loss, and additive white Gaussian noise. Performance analysis and numerical results are given.**

***Index Terms*—Sensor network, cooperative communication, relay placement.**

## I. Introduction

WIRELESS sensor networks typically consist of a large number of small, power-limited sensors distributed over a planar geographic area. In some scenarios, the sensors collect information which is transmitted to a single receiver for further analysis. A small number of radio relays with additional processing and communications capabilities can be strategically placed to help improve system performance. Two important problems we consider here are to position the relays and to determine, for each sensor, which relay should rebroadcast its signal.

Previous studies of relay placement have considered various optimization criteria and communication models. Some have focused on the coverage of the network (e.g., Balam and Gibson [2]; Chen, Wang, and Liang [4]; Cortés, Martiínez, Karataş, and Bullo [7]; Koutsopoulos, Toumpis, and Tassiulas [13]; Liu and Mohapatra [14]; Mao and Wu [15]; Suomela [22]; Tan, Lozano, Xi, and Sheng [23]). In [13] communication errors are modeled by a fixed probability of error without incorporating physical considerations; otherwise, communications are assumed to be error-free. Such studies often directly use the source coding technique known as the Lloyd algorithm (e.g., see [9]), which is sub-optimal for relay placement. Two other optimization criteria are network lifetime and energy usage, with energy modeled as an increasing function of distance and with error-free communications (e.g., Ergen and Varaiya [8]; Hou, Shi, Sherali, and Midkiff [11]; Iranli, Maleki, and Pedram [12]; Pan, Cai, Hou, Shi, and Shen [17]). Models incorporating fading and/or path loss have been used with criteria such as error probability, outage probability, and throughput, typically with simplifications such as single-sensor or single-relay networks (e.g., Cho and Yang [5]; So and Liang [21]; Sadek, Han, and Liu [20]). The majority of the above approaches do not include diversity. Those that do often do not focus on optimal relay location and use restricted networks with only a single source and/or a single relay (e.g., Ong and Motani [16]; Chen and Laneman [3]). These previous studies offer valuable insight; however, the communication and/or network models used are typically simplified.

In this work, we attempt to position the relays and determine which relay should rebroadcast each sensor's transmissions in order to minimize the average probability of error. We use a more elaborate communications model which includes path loss, fading, additive white Gaussian noise, and diversity. We use a network model in which all relays either use amplify-and-forward or decode-and-forward communications. Each sensor in the network transmits information to the receiver both directly and through a single-hop relay path. The receiver uses the two received signals to achieve diversity. Sensors identify themselves in transmissions and relays know for which sensors they are responsible. We assume TDMA communications by sensors and relays so that there is (ideally) no transmission interference. While such interference, due to effects such as multipath and imperfect frame synchronization, can be incorporated into our model, it is out of the scope of this paper.

We present an algorithm that determines relay placement and assigns each sensor to a relay. We refer to this algorithm as the *relay placement algorithm*. The algorithm has some similarity to the Lloyd algorithm. We describe geometrically, with respect to fixed relay positions, the sets of locations in the plane in which sensors are (optimally) assigned to the same relay, and give performance results based on these analyses and using numerical computations.

In Section II, we specify communications models and determine error probabilities. In Section III, we present our relay placement algorithm. In Section IV, we give analytic descriptions of optimal sensor regions (with respect to fixed relay positions). In Section V, we present numerical results. In Section VI, we summarize our work and provide ideas for future consideration.

## II. Communications Model and Performance Measure

### A. Signal, Channel, and Receiver Models

In a sensor network, we refer to sensors, relays, and the receiver as *nodes*. We assume that transmission of $b_i \in \{-1, 1\}$ by node $i$ uses the binary phase shift keyed (BPSK) signal $s_i(t)$, and we denote the transmission energy per bit by $E_i$.

Manuscript received August 4, 2008; revised May 8, 2009; accepted June 22, 2009. The associate editor coordinating the review of this paper and approving it for publication was Q. Zhang.

The authors are with the Department of Electrical and Computer Engineering, University of California, San Diego, La Jolla, CA 92093-0407 (e-mail: jcannons@code.ucsd.edu, milstein@ece.ucsd.edu, zeger@ucsd.edu).

This work was supported by the Air Force Office of Scientific Research award FA9550-06-1-0210, the National Science Foundation, and the UCSD Center for Wireless Communications.

Digital Object Identifier 10.1109/TWC.2009.081036

In particular, we assume all sensor nodes transmit at the same energy per bit, denoted by $E_{\mathrm{Tx}}$. The communications channel model includes path loss, additive white Gaussian noise (AWGN), and fading. Let $L_{i,j}$ denote the far field path loss between two nodes $i$ and $j$ that are separated by a distance $d_{i,j}$ (in meters). We consider the free-space law model (e.g., see [19, pp. 70 – 73]) for which[1]

$$L_{i,j} = \frac{F_2}{d_{i,j}^2} \tag{1}$$

where:

$F_2 = \frac{\lambda^2}{16\pi^2}$ (in meters$^2$)

$\lambda = c/f_0$ is the wavelength of the carrier wave (in meters)

$c = 3 \cdot 10^8$ is the speed of light (in meters/second)

$f_0$ is the frequency of the carrier wave (in Hz).

The formula in (1) is impractical in the near field, since $L_{i,j} \to \infty$ as $d_{i,j} \to 0$. Comaniciu and Poor [6] addressed this issue by not allowing transmissions at distances less than $\lambda$. Ong and Motani [16] allow near field transmissions by proposing a modified model with path loss

$$L_{i,j} = \frac{F_2}{(1 + d_{i,j})^2}. \tag{2}$$

We assume additive white Gaussian noise $n_j(t)$ at the receiving antenna of node $j$. The noise has one-sided power spectral density $N_0$ (in W/Hz). We assume the channel fading (excluding path loss) between nodes $i$ and $j$ is a random variable $h_{i,j}$ with Rayleigh density

$$p_{h_{i,j}}(h) = (h/\sigma^2)e^{-h^2/(2\sigma^2)} \quad (h \geq 0). \tag{3}$$

We also consider AWGN channels (which is equivalent to assuming $h_{i,j} = 1$ for all $i, j$).

Let the signal received after transmission from node $i$ to node $j$ be denoted by $r_{i,j}(t)$. Combining the signal and channel models, we have

$$r_{i,j}(t) = \sqrt{L_{i,j}}\, h_{i,j} s_i(t) + n_j(t).$$

The received energy per bit without fading is

$$E_j = E_i L_{i,j}.$$

We assume demodulation at a receiving node is performed by applying a matched filter to obtain the test statistic. Diversity is achieved at the receiver by making a decision based on the test statistic that combines the two received versions (i.e., direct and relayed) of the transmission from a given sensor. We assume the receiver uses selection combining, in which only the better of the two incoming signals (determined by a measurable quantity such as the received signal-to-noise-ratio (SNR)) is used to detect the transmitted bit.

### *B. Path Probability of Error*

For each sensor, we determine the probability of error along the direct path from the sensor to the receiver and along single-hop[2] relay paths, for both amplify-and-forward and decode-and-forward protocols. Let $\mathbf{x} \in \mathbb{R}^2$ denote a transmitter position and let $\mathrm{Rx}$ denote the receiver. We consider transmission paths of the forms $(\mathbf{x}, \mathrm{Rx})$, $(\mathbf{x}, i)$, $(i, \mathrm{Rx})$, and $(\mathbf{x}, i, \mathrm{Rx})$, where $i$ denotes a relay index. For each such path $q$, let:

$$\mathrm{SNR}_H^q = \text{end-to-end SNR, conditioned on fades} \tag{4}$$

$$P_{e|H}^q = \text{end-to-end error probability, conditioned on fades} \tag{5}$$

$$\mathrm{SNR}^q = \text{end-to-end SNR} \tag{6}$$

$$P_e^q = \text{end-to-end error probability.} \tag{7}$$

For AWGN channels, we take $\mathrm{SNR}^q$ and $P_e^q$ to be the SNR and error probability, respectively, when the signal is degraded only by path loss and receiver antenna noise. For fading channels, we assume $\mathrm{SNR}^q$ and $P_e^q$ to be averaged over the fades. Note that the signal-to-noise ratios only apply to direct paths and paths using amplify-and-forward relays. Finally, denote the Gaussian error function by

$$Q(x) = \frac{1}{\sqrt{2\pi}} \int_x^\infty e^{-y^2/2} dy.$$

*1) Direct Path (i.e., unrelayed):* For Rayleigh fading, we have (e.g., see [18, pp. 817 – 818])

$$\begin{aligned} \mathrm{SNR}^{(\mathbf{x},\mathrm{Rx})} &= \frac{4\sigma^2 E_{\mathrm{Tx}} L_{\mathbf{x},\mathrm{Rx}}}{N_0} \\ \mathrm{SNR}^{(\mathbf{x},i)} &= \frac{4\sigma^2 E_{\mathrm{Tx}} L_{\mathbf{x},i}}{N_0} \\ \mathrm{SNR}^{(i,\mathrm{Rx})} &= \frac{4\sigma^2 E_i L_{i,\mathrm{Rx}}}{N_0}; \end{aligned} \tag{8}$$

$$P_e^{(\mathbf{x},\mathrm{Rx})} = \frac{1}{2}\left(1 - \left(1 + \frac{2}{\mathrm{SNR}^{(\mathbf{x},\mathrm{Rx})}}\right)^{-1/2}\right). \tag{9}$$

For AWGN channels, we have (e.g., see [18, pp. 255 – 256])

$$\begin{aligned} \mathrm{SNR}^{(\mathbf{x},\mathrm{Rx})} &= \frac{2E_{\mathrm{Tx}} L_{\mathbf{x},\mathrm{Rx}}}{N_0} \\ \mathrm{SNR}^{(\mathbf{x},i)} &= \frac{2E_{\mathrm{Tx}} L_{\mathbf{x},i}}{N_0} \\ \mathrm{SNR}^{(i,\mathrm{Rx})} &= \frac{2E_i L_{i,\mathrm{Rx}}}{N_0}; \end{aligned} \tag{10}$$

$$P_e^{(\mathbf{x},\mathrm{Rx})} = Q\left(\sqrt{\mathrm{SNR}^{(\mathbf{x},\mathrm{Rx})}}\right). \tag{11}$$

Note that analogous formulas to those in (9) and (11) can be given for $P_e^{(\mathbf{x},i)}$ and $P_e^{(i,\mathrm{Rx})}$.

*2) Relay Path with Amplify-and-Forward:* For amplify-and-forward relays,[3] the system is linear. Denote the gain by $G$. Conditioning on the fading values, we have (e.g., see [10])

$$\mathrm{SNR}_H^{(\mathbf{x},i,\mathrm{Rx})} = \frac{h_{\mathbf{x},i}^2 h_{i,\mathrm{Rx}}^2 E_{\mathrm{Tx}}/N_0}{B_i h_{i,\mathrm{Rx}}^2 + D_i} \tag{12}$$

$$P_{e|H}^{(\mathbf{x},i,\mathrm{Rx})} = Q\left(\sqrt{\mathrm{SNR}_h^{(\mathbf{x},i,\mathrm{Rx})}}\right) \tag{13}$$

$$\text{where} \quad B_i = \frac{1}{2L_{\mathbf{x},i}}; \qquad D_i = \frac{1}{2G^2 L_{\mathbf{x},i} L_{i,\mathrm{Rx}}}. \tag{14}$$

[1]Much of the material of this paper can be generalized by replacing the path loss exponent 2 by any positive, even integer, and $F_2$ by a corresponding constant.

[2]Computing the probabilities of error for the more general case of multi-hop relay paths is straightforward.

[3]By *amplify-and-forward relays* we specifically mean that a received signal is multiplied by a constant gain factor and then transmitted.

Then, the end-to-end probability of error, averaged over the fades, is

$$\begin{aligned}
&P_e^{(\mathbf{x},i,\mathrm{Rx})} \\
&= \int_0^\infty \int_0^\infty P_{e|H}^{(\mathbf{x},i,\mathrm{Rx})} p_H\left(h_{\mathbf{x},i}\right) p_H\left(h_{i,\mathrm{Rx}}\right) dh_{\mathbf{x},i}\, dh_{i,\mathrm{Rx}} \\
&= \int_0^\infty \int_0^\infty Q\left(\sqrt{\frac{h_{\mathbf{x},i}^2 h_{i,\mathrm{Rx}}^2 E_{\mathrm{Tx}}/N_0}{B_i h_{i,\mathrm{Rx}}^2 + D_i}}\right) \frac{h_{\mathbf{x},i}}{\sigma^2} \\
&\qquad \cdot \exp\left\{-\frac{h_{\mathbf{x},i}^2}{2\sigma^2}\right\} \frac{h_{i,\mathrm{Rx}}}{\sigma^2} \\
&\qquad \cdot \exp\left\{-\frac{h_{i,\mathrm{Rx}}^2}{2\sigma^2}\right\} dh_{\mathbf{x},i}\, dh_{i,\mathrm{Rx}} \\
&\qquad\qquad [\text{from (13), (12), (3)}] \\
&= \frac{1}{2} - \frac{D_i N_0/E_{\mathrm{Tx}}}{4\sigma\left(\sigma^2 + B_i N_0/E_{\mathrm{Tx}}\right)^{3/2}} \left[\int_0^\infty \sqrt{\frac{t}{t+1}} \right. \\
&\qquad \left. \cdot \exp\left\{-t\left(\frac{D_i N_0/E_{\mathrm{Tx}}}{2\sigma^2\left(\sigma^2 + B_i N_0/E_{\mathrm{Tx}}\right)}\right)\right\} dt\right] \\
&= \frac{1}{2} - \frac{D_i \sqrt{\pi} N_0/E_{\mathrm{Tx}}}{8\sigma\left(\sigma^2 + B_i N_0/E_{\mathrm{Tx}}\right)^{3/2}} \\
&\qquad \cdot U\left(\frac{3}{2}, 2, \frac{D_i N_0/E_{\mathrm{Tx}}}{2\sigma^2\left(\sigma^2 + B_i N_0/E_{\mathrm{Tx}}\right)}\right) \qquad (15)
\end{aligned}$$

where $U(a,b,z)$ denotes the confluent hypergeometric function of the second kind [1, p. 505] (also known as Kummer's function of the second kind), i.e.,

$$U(a,b,z) = \frac{1}{\Gamma(a)} \int_0^\infty e^{-zt} t^{a-1} (1+t)^{b-a-1}\, dt.$$

For AWGN channels, we have

$$\mathrm{SNR}^{(\mathbf{x},i,\mathrm{Rx})} = \frac{E_{\mathrm{Tx}}/N_0}{B_i + D_i} \qquad [\text{from (12)}] \qquad (16)$$

$$P_e^{(\mathbf{x},i,\mathrm{Rx})} = Q\left(\sqrt{\mathrm{SNR}^{(\mathbf{x},i,\mathrm{Rx})}}\right). \qquad (17)$$

*3) Relay Path with Decode-and-Forward:* For decode-and-forward relays,[4] the signal at the receiver is not a linear function of the transmitted signal (i.e., the system is not linear), as the relay makes a hard decision based on its incoming data. A decoding error occurs at the receiver if and only if exactly one decoding error is made along the relay path, i.e.,

$$P_e^{(\mathbf{x},i,\mathrm{Rx})} = P_e^{(\mathbf{x},i)}\left(1 - P_e^{(i,\mathrm{Rx})}\right) + P_e^{(i,\mathrm{Rx})}\left(1 - P_e^{(\mathbf{x},i)}\right). \qquad (18)$$

In particular, for Rayleigh fading,

$$\begin{aligned}
P_e^{(\mathbf{x},i,\mathrm{Rx})} &= \frac{1}{4}\left(1 - \left(1 + \frac{2}{\mathrm{SNR}^{(\mathbf{x},i)}}\right)^{-1/2}\right) \\
&\qquad \cdot \left(1 + \left(1 + \frac{2}{\mathrm{SNR}^{(i,\mathrm{Rx})}}\right)^{-1/2}\right) \\
&\quad + \frac{1}{4}\left(1 - \left(1 + \frac{2}{\mathrm{SNR}^{(i,\mathrm{Rx})}}\right)^{-1/2}\right) \\
&\qquad \cdot \left(1 + \left(1 + \frac{2}{\mathrm{SNR}^{(\mathbf{x},i)}}\right)^{-1/2}\right). \\
&\qquad\qquad [\text{from (9)}] \qquad (19)
\end{aligned}$$

Similarly, one can substitute (11) into (18) for AWGN channels.

## III. Path Selection and Relay Placement Algorithm

### A. Definitions

We define a *sensor network with relays* to be a collection of sensors and relays in $\mathbb{R}^2$, together with a single receiver at the origin, where each sensor transmits to the receiver both directly and through some predesignated relay for the sensor, and the system performance is evaluated using the measure given in (20). Specifically, let $\mathbf{x}_1, \ldots, \mathbf{x}_M \in \mathbb{R}^2$ be the sensor positions and let $\mathbf{y}_1, \ldots, \mathbf{y}_N \in \mathbb{R}^2$ be the relay positions. Typically, $N \ll M$. Let

$$p : \mathbb{R}^2 \to \{1, \ldots, N\}$$

be a *sensor-relay assignment*, where $p(\mathbf{x}) = i$ means that if a sensor were located at position $\mathbf{x}$, then it would be assigned to relay $\mathbf{y}_i$. Let $\mathcal{S}$ be a bounded subset of $\mathbb{R}^2$. Throughout both this section and Section IV we will consider sensor-relay assignments whose domains are restricted to $\mathcal{S}$ (since the number of sensors is finite). Let the *sensor-averaged probability of error* be given by

$$\frac{1}{M} \sum_{s=1}^{M} P_e^{(\mathbf{x}_s, p(\mathbf{x}_s), \mathrm{Rx})}. \qquad (20)$$

Note that (20) depends on the relay locations through the sensor-relay assignment $p$.

### B. Overview of the Proposed Algorithm

The proposed iterative algorithm attempts to minimize the sensor-averaged probability of error[5] over all choices of relay positions $\mathbf{y}_1, \ldots, \mathbf{y}_N$ and sensor-relay assignments $p$. The algorithm operates in two phases. First, the relay positions are fixed and the best sensor-relay assignment is determined; second, the sensor-relay assignment is fixed and the best relay positions are determined. An initial placement of the relays is made either randomly or using some heuristic. The two phases are repeated until the quantity in (20) has converged within some threshold.

[4]By *decode-and-forward relays* we specifically mean that a single symbol is demodulated and then remodulated; no additional decoding is performed (e.g., of channel codes).

[5]Here we minimize (20); however, the algorithm can be adapted to minimize other performance measures.

### C. Phase 1: Optimal Sensor-Relay Assignment

In the first phase, we assume the relay positions $\mathbf{y}_1, \ldots, \mathbf{y}_N$ are fixed and choose an optimal[6] sensor-relay assignment $p^*$, in the sense of minimizing (20). This choice can be made using an exhaustive search in which all possible sensor-relay assignments are examined. A sensor-relay assignment induces a partition of $\mathcal{S}$ into subsets for which all sensors in any such subset are assigned to the same relay. For each relay $\mathbf{y}_i$, let $\sigma_i$ be the set of all points $\mathbf{x} \in \mathcal{S}$ such that if a sensor were located at position $\mathbf{x}$, then the optimally assigned relay that rebroadcasts its transmissions would be $\mathbf{y}_i$, i.e.,

$$\sigma_i = \{\mathbf{x} \in \mathcal{S} : p^*(\mathbf{x}) = i\}.$$

We call $\sigma_i$ the $i^{th}$ *optimal sensor region* (with respect to the fixed relay positions).

### D. Phase 2: Optimal Relay Placement

In the second phase, we assume the sensor-relay assignment is fixed and choose optimal[7] relay positions in the sense of minimizing (20). Numerical techniques can be used to determine such optimal relay positions. For the first three invocations of phase 2 in the iterative algorithm, we used an efficient (but slightly sub-optimal) numerical approach that quantizes a bounded subset of $\mathbb{R}^2$ into gridpoints. For a given relay, the best gridpoint was selected as the new location for the relay. For subsequent invocations of phase 2, the restriction of lying on a gridpoint was removed and a steepest descent technique was used to refine the relay locations.

## IV. Geometric Descriptions of Phase 1 Optimal Sensor Regions

We now geometrically describe the optimal sensor regions used in Phase 1 of the algorithm by considering specific relay protocols and channel models. In particular, we examine amplify-and-forward and decode-and-forward relaying protocols in conjunction with either AWGN channels or Rayleigh fading channels. We define the *internal boundary* of any optimal sensor region $\sigma_i$ to be the portion of the boundary of $\sigma_i$ that does not lie on the boundary of $\mathcal{S}$. For amplify-and-forward and AWGN channels, we show that the internal boundary of each optimal sensor region consists only of circular arcs. For the other three combinations of relay protocol and channel type, we show that as the transmission energies of sensors and relays grow, the internal boundary of each optimal sensor region converges to finite combinations of circular arcs and/or line segments.

For each pair of relays $(\mathbf{y}_i, \mathbf{y}_j)$, let $\sigma_{i,j}$ be the set of all points $\mathbf{x} \in \mathcal{S}$ such that if a sensor were located at position $\mathbf{x}$, then its average probability of error using relay $\mathbf{y}_i$ would be smaller than that using relay $\mathbf{y}_j$, i.e.,

$$\sigma_{i,j} = \left\{\mathbf{x} \in \mathcal{S} : P_e^{(\mathbf{x},i,\mathrm{Rx})} < P_e^{(\mathbf{x},j,\mathrm{Rx})}\right\}. \tag{21}$$

[6]This choice may not be unique, but we select one such minimizing assignment here. Also, the optimality of $p^*$ here depends only on the values $p^*(\mathbf{x}_1), \ldots, p^*(\mathbf{x}_M)$.

[7]This choice may not be unique, but we select one such set of positions here.

Note that $\sigma_{i,j} = \mathcal{S} - \sigma_{j,i}$. Then, for the given set of relay positions, we have

$$\sigma_i = \bigcap_{\substack{j=1 \\ j \neq i}}^{N} \sigma_{i,j} \tag{22}$$

since

$$p^*(\mathbf{x}) = \underset{j \in \{1,\ldots,N\}}{\operatorname{argmin}} P_e^{(\mathbf{x},j,\mathrm{Rx})}.$$

Furthermore, for a suitably chosen constant $C > 0$, in order to facilitate analysis, we modify (2) to[8]

$$L_{i,j} = \frac{F_2}{C + d_{i,j}^2}. \tag{23}$$

### A. Amplify-and-Forward with AWGN Channels

**Theorem IV.1.** *Consider a sensor network with amplify-and-forward relays and AWGN channels. Then, the internal boundary of each optimal sensor region consists of circular arcs.*

*Proof:* See Appendix A. ∎

Figure 1a shows the optimal sensor regions $\sigma_1, \sigma_2, \sigma_3$, and $\sigma_4$, for $N = 4$ randomly placed amplify-and-forward relays with AWGN channels and system parameter values

$$G = 65 \text{ dB}$$
$$f_0 = 900 \text{ MHz}$$
$$C = 1.$$

### B. Decode-and-Forward with AWGN Channels

**Theorem IV.2.** *Consider a sensor network with decode-and-forward relays and AWGN channels, and, for all relays $i$, let $E_i/N_0 \to \infty$ and $E_{\mathrm{Tx}}/N_0 \to \infty$ such that $(E_i/N_0)/(E_{\mathrm{Tx}}/N_0)$ has a limit. Then, the internal boundary of each optimal sensor region consists asymptotically of circular arcs and line segments.*

*Proof:* See Appendix B. ∎

Figure 1b shows the asymptotically-optimal sensor regions $\sigma_1, \sigma_2, \sigma_3$, and $\sigma_4$, for $N = 4$ randomly placed decode-and-forward relays with AWGN channels and system parameter values

$$C = 1$$
$$E_{\mathrm{Rx}}/N_0|_{d=50\text{ m}} = 5 \text{ dB}$$
$$E_i/N_0 = 2E_{\mathrm{Tx}}/N_0 \text{ for all relays } \mathbf{y}_i.$$

### C. Amplify-and-Forward with Rayleigh Fading Channels

We define the *nearest-neighbor region* of a relay $\mathbf{y}_i$ to be

$$\{\mathbf{x} \in \mathcal{S} : \forall j,\ \|\mathbf{x} - \mathbf{y}_i\| < \|\mathbf{x} - \mathbf{y}_j\|\}$$

where ties (i.e., $\|\mathbf{x} - \mathbf{y}_i\| = \|\mathbf{x} - \mathbf{y}_j\|$) are broken arbitrarily. The interiors of these regions are convex polygons intersected with $\mathcal{S}$.

[8]Numerical results confirm that (23) is a close approximation of (2) for our parameters of interest.

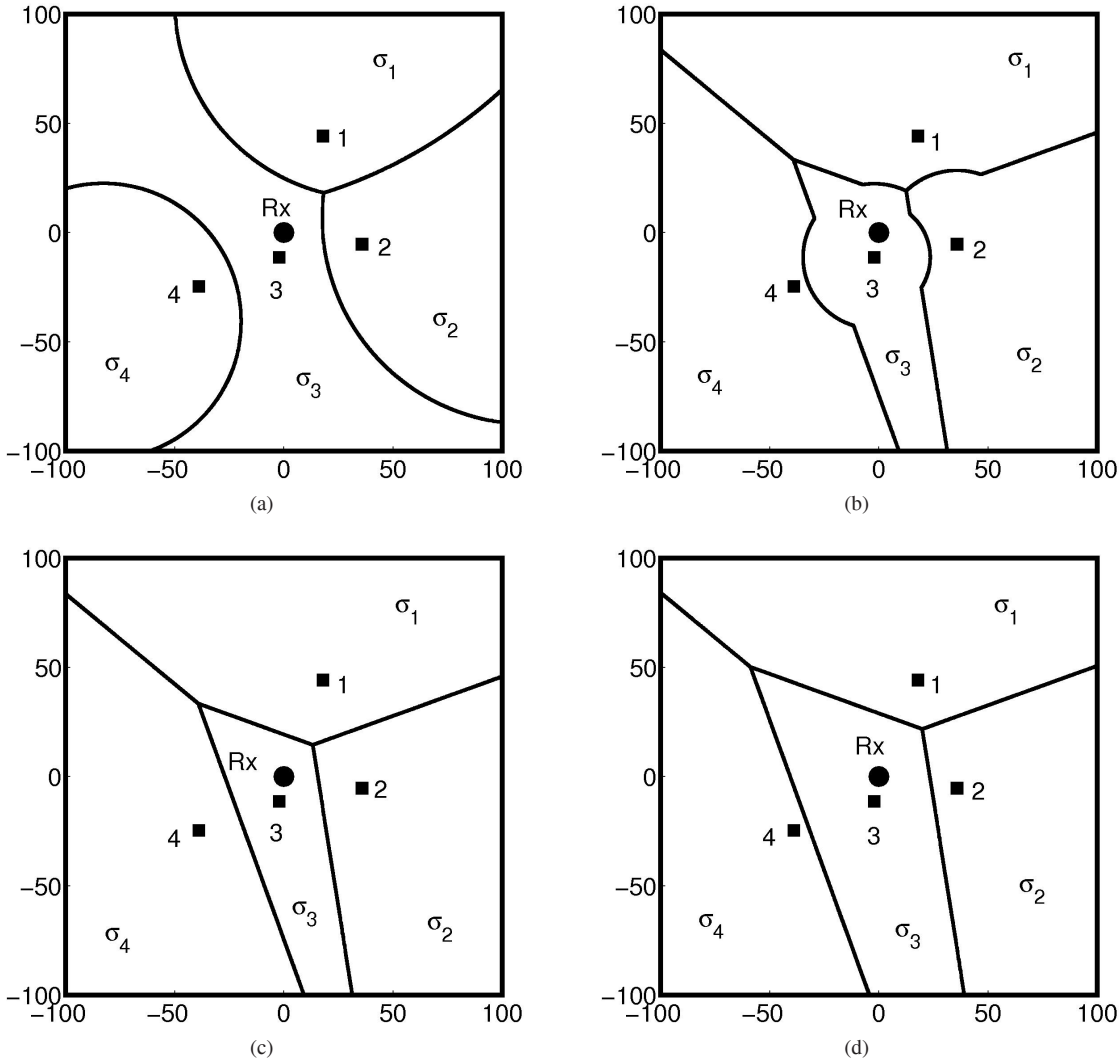


Fig. 1. Sensor regions $\sigma_1$, $\sigma_2$, $\sigma_3$, and $\sigma_4$ for 4 randomly placed relays. Each relay $i \in \{1, 2, 3, 4\}$ is denoted by a filled square labeled $i$, while the receiver is denoted by a filled circle labeled Rx. Sensors are distributed as a square grid over $\pm 100$ meters in each dimension. The sensor regions are either optimal or asymptotically-optimal as described in (a) Theorem IV.1 (amplify-and-forward relays and AWGN channels), (b) Theorem IV.2 (decode-and-forward relays and AWGN channels with high $E_{\mathrm{Tx}}/N_0$ and $E_i/N_0$), (c) Theorem IV.3 (amplify-and-forward relays and Rayleigh fading channels with high $E_{\mathrm{Tx}}/N_0$), and (d) Theorem IV.4 (decode-and-forward relays and Rayleigh fading channels) with high $E_{\mathrm{Tx}}/N_0$ and $E_i/N_0$).

**Theorem IV.3.** *Consider a sensor network with amplify-and-forward relays and Rayleigh fading channels, and let $E_{\mathrm{Tx}}/N_0 \to \infty$. Then, each optimal sensor region is asymptotically equal to the corresponding relay's nearest-neighbor region.*

*Proof:* See Appendix C. ■

Figure 1c shows the asymptotically-optimal sensor regions $\sigma_1, \sigma_2, \sigma_3$, and $\sigma_4$, for $N = 4$ randomly placed amplify-and-forward relays with Rayleigh fading channels.

### D. Decode-and-Forward with Rayleigh Fading Channels

**Theorem IV.4.** *Consider a sensor network with decode-and-forward relays and Rayleigh fading channels, and, for all relays $i$, let $E_i/N_0 \to \infty$ and $E_{\mathrm{Tx}}/N_0 \to \infty$ such that $(E_i/N_0)/(E_{\mathrm{Tx}}/N_0)$ has a limit. Then, the internal boundary of each optimal sensor region is asymptotically piecewise linear.*

*Proof:* See Appendix D. ■

Note that if, for all relays $\mathbf{y}_i$, $E_i$ is a constant and $G_i = \infty$, then each optimal sensor region is asymptotically equal to the corresponding relay's nearest-neighbor regions, as was the case for amplify-and-forward relays and Rayleigh fading channels. In addition, we note that, while Theorem IV.4 considers the asymptotic case, we have empirically observed that the internal boundary of each optimal sensor region consists of line segments for a wide range of moderate parameter values.

Figure 1d shows the asymptotically-optimal sensor regions $\sigma_1, \sigma_2, \sigma_3$, and $\sigma_4$, for $N = 4$ randomly placed decode-and-forward relays with Rayleigh fading channels and system parameter values

$$C = 1$$
$$E_{\mathrm{Rx}}/N_0|_{d=50\ \mathrm{m}} = 5\ \mathrm{dB}$$
$$E_i/N_0 = 2E_{\mathrm{Tx}}/N_0 \text{ for all relays } \mathbf{y}_i.$$

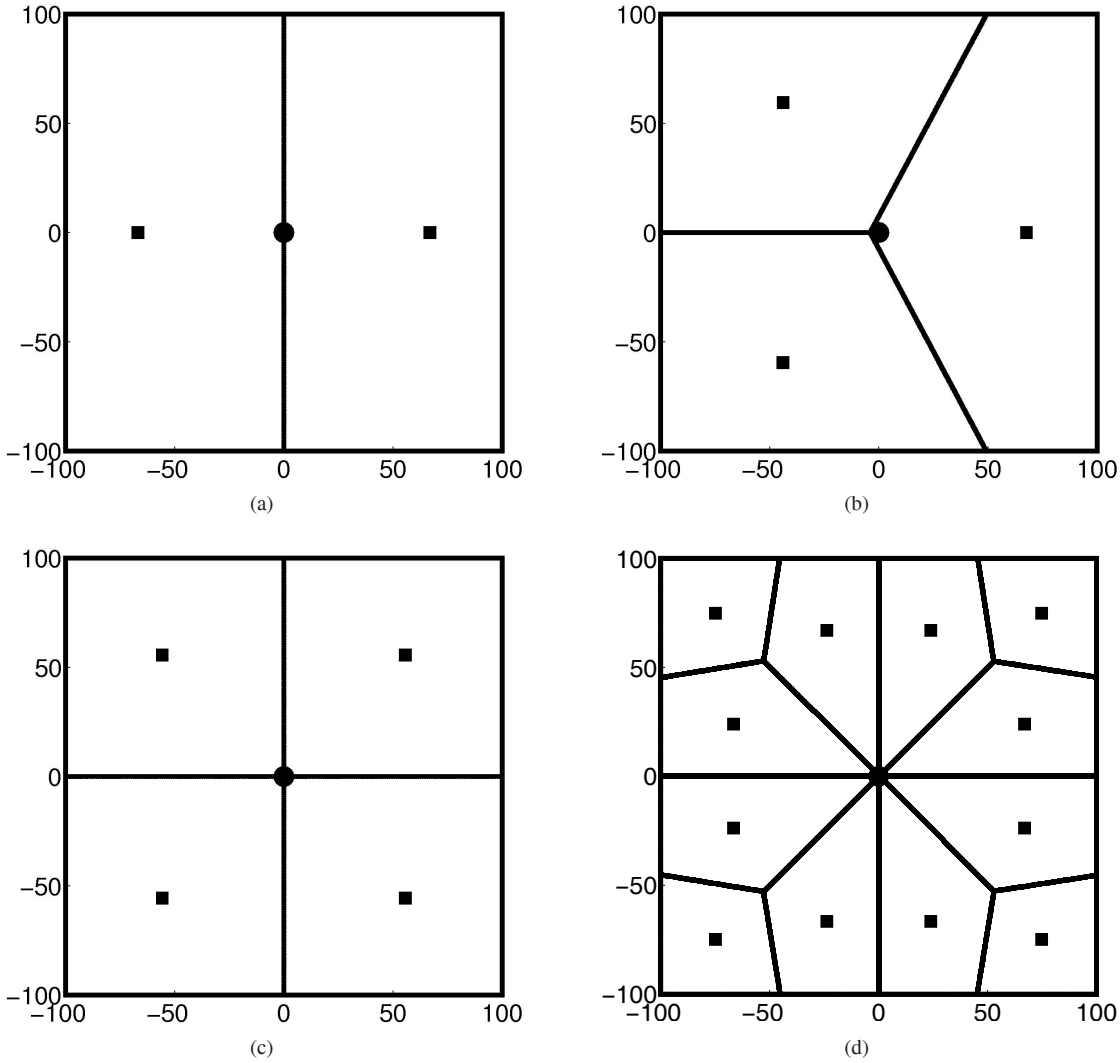


Fig. 2. Optimal sensor regions output by the algorithm for decode-and-forward relays and fading channels with $E_i = 100E_{\mathrm{Tx}}$, and $E_{\mathrm{Rx}}/N_0|_{d=50\ \mathrm{m}} = 10$ dB. Relays are denoted by squares and the receiver is located at $(0, 0)$. Sensors are distributed as a square grid over $\pm 100$ meters in each dimension. The number of relays is (a) $N = 2$, (b) $N = 3$, (c) $N = 4$, and (d) $N = 12$.

## V. Numerical Results for the Relay Placement Algorithm

The relay placement algorithm was implemented for both amplify-and-forward and decode-and-forward relays. The sensors were placed uniformly in a square of sidelength 100 m. For decode-and-forward and all relays $\mathbf{y}_i$, the energy $E_i$ was set to a constant which equalized the total output power of all relays for both amplify-and-forward and decode-and-forward. Specific numerical values for system variables were

$$\begin{aligned} f_0 &= 900\ \text{MHz} \\ \sigma &= \sqrt{2}/2 \\ M &= 10000 \\ C &= 1. \end{aligned}$$

In order to use the relay placement algorithm to produce good relay locations and sensor-relay assignments, we ran the algorithm 10 times. Each such run was initiated with a different random set of relay locations (uniformly distributed on the square $\mathcal{S}$) and used the sensor-averaged probability of error given in (20). For each of the 10 runs completed, 1000 simulations were performed with Rayleigh fading and diversity (selection combining) at the receiver. Different realizations of the fade values for the sensor network channels were chosen for each of the 1000 simulations. Of the 10 runs, the relay locations and sensor-relay assignments of the run with the lowest average probability of error over the 1000 simulations was chosen.

Figure 2 gives the algorithm output for 2, 3, 4, and 12 decode-and-forward relays with

$$\begin{aligned} E_{\mathrm{Rx}}/N_0|_{d=50\ \mathrm{m}} &= 10\ \text{dB} \\ E_i &= 100E_{\mathrm{Tx}} \end{aligned}$$

and using the exact error probability expressions. Relays are denoted by squares and the receiver is denoted by a circle at the origin. Boundaries between the optimal sensor regions are shown. For 2, 3, and 4 relays a symmetry is present, with each relay being responsible for approximately the same number of sensors. A symmetry is also present for 12 relays; here, however, eight relays are responsible for approximately the same number of sensors, and the remaining four relays are located near the corners of $\mathcal{S}$ to assist in transmissions

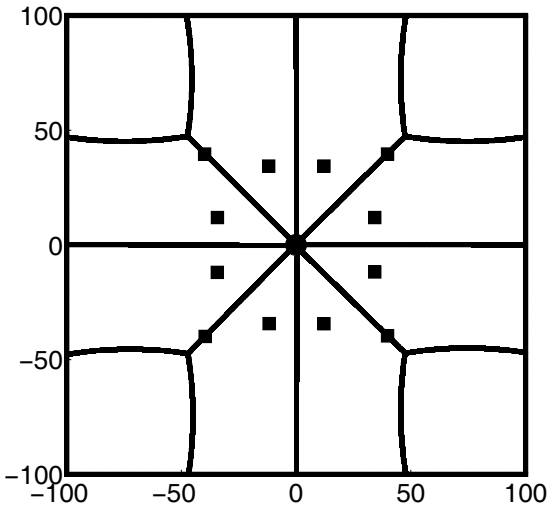


Fig. 3. Optimal sensor regions $\sigma_1, \ldots, \sigma_{12}$ output by the algorithm for decode-and-forward relays and fading channels with $N = 12$, $E_i = 1.26E_{\mathrm{Tx}}$, and $E_{\mathrm{Rx}}/N_0|_{d=50\ \mathrm{m}} = 5$ dB.

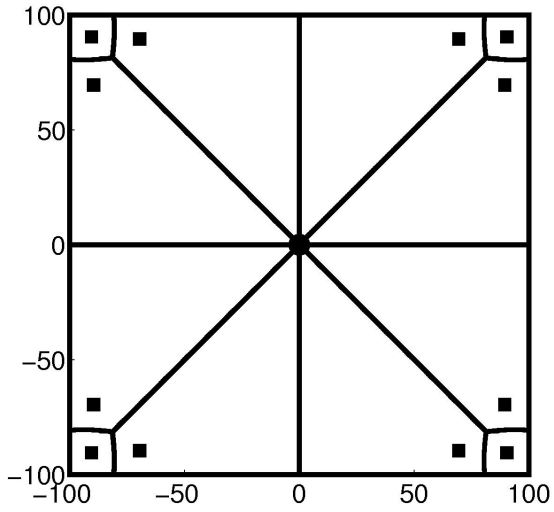


Fig. 4. Optimal sensor regions $\sigma_1, \ldots, \sigma_{12}$ output by the algorithm for amplify-and-forward relays and fading channels with $N = 12$, $G = 56$ dB, and $E_{\mathrm{Rx}}/N_0|_{d=50\ \mathrm{m}} = 5$ dB.

experiencing the largest path loss due to distance. Such symmetries reflect the use of relay positions which attempt to balance the performance of individual sensors in order to minimize the overall average probability of error. Since the relays transmit at higher energies than the sensors, the probability of detection error is reduced by reducing path loss before a relay rebroadcasts a sensor's signal, rather than after the relay rebroadcasts the signal (even at the expense of possibly greater path loss from the relay to the receiver). Thus, some sensors actually transmit "away" from the receiver to their associated relay. The asymptotically-optimal sensor regions closely matched those for the exact error probability expressions, which is expected due to the large value selected for $E_i$. In addition, the results for amplify-and-forward relays were quite similar, with the relays lying closer to the corners of $\mathcal{S}$ for the 2 and 3 relay cases, and the corner regions displaying slightly curved boundaries for 12 relays. With the exception of this curvature, the asymptotic regions closely matched those from the exact error probability expressions. This similarity between decode-and-forward and amplify-and-forward relays is expected due to the large value selected for $E_i$.

Figures 3 and 4 give the algorithm output for 12 decode-and-forward and amplify-and-forward relays, respectively, with

$$E_{\mathrm{Rx}}/N_0|_{d=50\ \mathrm{m}} = 5\ \mathrm{dB}$$
$$E_i = 1.26E_{\mathrm{Tx}}$$

and using the exact error probability expressions. For decode-and-forward relays, the results are similar to those in Figure 2d; however the relays are located much closer to the receiver due to their decreased transmission energy, and the corner regions of $\mathcal{S}$ exhibit slightly curved boundaries. For amplify-and-forward relays, the relays are located much closer to the corners since, with lower gain, the relays are less effective and thus primarily assist those sensors with the largest path loss.

The maximum, average, and median of the sensor probabilities of error for all of the above figures are given in Table I. The sensor error probability is lowest for sensors that are closest to the relays, and increases with distance.

TABLE I
SENSOR PROBABILITY OF ERROR VALUES.

| Figure | Max. $P_e$ | Avg. $P_e$ | Median $P_e$ |
|---|---|---|---|
| 2a | $7.3 \cdot 10^{-2}$ | $1.8 \cdot 10^{-2}$ | $1.2 \cdot 10^{-2}$ |
| 2b | $6.9 \cdot 10^{-2}$ | $1.2 \cdot 10^{-2}$ | $7.2 \cdot 10^{-3}$ |
| 2c | $3.3 \cdot 10^{-2}$ | $7.0 \cdot 10^{-3}$ | $5.1 \cdot 10^{-3}$ |
| 2d | $1.4 \cdot 10^{-2}$ | $2.8 \cdot 10^{-3}$ | $2.3 \cdot 10^{-3}$ |
| 3 | $2.0 \cdot 10^{-1}$ | $6.2 \cdot 10^{-2}$ | $5.6 \cdot 10^{-2}$ |
| 4 | $1.7 \cdot 10^{-1}$ | $9.9 \cdot 10^{-2}$ | $1.1 \cdot 10^{-1}$ |

## VI. CONCLUSIONS

This paper presented an algorithm for amplify-and-forward and decode-and-forward relay placement and sensor assignment in wireless sensor networks that attempts to minimize the average probability of error. Communications were modeled using path loss, fading, AWGN, and diversity combining. We determined the geometric shapes of regions for which sensors would be optimally assigned to the same relay (for a given set of relay locations), in some instances for the asymptotic case of the ratios of the transmission energies to the noise power spectral density growing without bound. Numerical results showing the algorithm output were presented. The asymptotic regions were seen to closely match the regions obtained using exact expressions. The complexity of the implemented relay placement algorithm is roughly as follows: determining sensor-relay assignments (Phase 1) is proportional to the number of sensors times the number of relays, and relay placement (Phase 2) using the gridpoint approach is proportional to the number of gridpoints times the sum of the number of relays and sensors. Reducing this complexity would be an interesting topic for future research.

A number of extensions to the relay placement algorithm could be incorporated to enhance the system model. Some

such enhancements are multi-hop relay paths, more sophisticated diversity combining, power constraints, sensor priorities, and sensor information correlation.

## APPENDIX A: PROOF OF THEOREM IV.1

For any distinct relays $\mathbf{y}_i$ and $\mathbf{y}_j$, let

$$K_i = \frac{1}{G^2F_2 + C + \|\mathbf{y}_i\|^2}; \qquad \gamma_{i,j} = \frac{K_i}{K_i - K_j}. \tag{24}$$

Note that for fixed gain $G$, $K_i \neq K_j$ since we assume $\mathbf{y}_i \neq \mathbf{y}_j$. Then, we have

$$\begin{aligned}
\sigma_{i,j} &= \left\{\mathbf{x} \in \mathcal{S} : P_e^{(\mathbf{x},i,\mathrm{Rx})} < P_e^{(\mathbf{x},j,\mathrm{Rx})}\right\} \\
&= \left\{\mathbf{x} \in \mathcal{S} : \frac{K_i}{C + \|\mathbf{x} - \mathbf{y}_i\|^2} > \frac{K_j}{C + \|\mathbf{x} - \mathbf{y}_j\|^2}\right\} \\
&\qquad \text{[from (17),(16),(14),(23),(24)]} \qquad (25) \\
&= \left\{\mathbf{x} \in \mathcal{S} : \|\mathbf{x} - (1-\gamma_{i,j})\,\mathbf{y}_i - \gamma_{i,j}\mathbf{y}_j\|^2 \underset{K_i-K_j<0}{\overset{K_i-K_j>0}{\gtrless}} \right. \\
&\qquad \left. \gamma_{i,j}\,(\gamma_{i,j}-1)\,\|\mathbf{y}_i - \mathbf{y}_j\|^2 - C\right\} \\
&\qquad \text{[from (24)]} \qquad (26)
\end{aligned}$$

where the notation

$$\overset{K_i-K_j>0}{\gtrless}$$
$$K_i-K_j<0$$

indicates that "$>$" should be used if $K_i - K_j > 0$, and "$<$" if $K_i - K_j < 0$. By (26), the set $\sigma_{i,j}$ is either the interior or the exterior of a circle (depending on the sign of $K_i - K_j$). Applying (22) completes the proof.

## APPENDIX B: PROOF OF THEOREM IV.2

**Lemma B.1** (e.g., see [25, pp. 82 – 83], [24, pp. 37 – 39])**.** *For all $x > 0$,*

$$\left(1 - \frac{1}{x^2}\right)\left(\frac{e^{-x^2/2}}{\sqrt{2\pi}x}\right) \leq Q(x) \leq \frac{e^{-x^2/2}}{\sqrt{2\pi}x}.$$

**Lemma B.2.** *Let $\epsilon > 0$ and*

$$L_{x,y} = \frac{Q\left(\sqrt{x}\right) + Q\left(\sqrt{y}\right) - 2Q\left(\sqrt{x}\right)Q\left(\sqrt{y}\right)}{\max\left(\frac{e^{-x/2}}{\sqrt{2\pi x}}, \frac{e^{-y/2}}{\sqrt{2\pi y}}\right)}.$$

*Then, $1 - \epsilon \leq L_{x,y} \leq 2$ for $x$ and $y$ sufficiently large.*

*Proof:* For the lower bound, we have

$$\begin{aligned}
L_{x,y} &\geq \frac{\frac{e^{-x/2}}{\sqrt{2\pi x}} + \frac{e^{-y/2}}{\sqrt{2\pi y}}}{\frac{e^{-x/2}}{\sqrt{2\pi x}} + \frac{e^{-y/2}}{\sqrt{2\pi y}}} - \frac{\frac{e^{-x/2}}{x\sqrt{2\pi x}} + \frac{e^{-y/2}}{y\sqrt{2\pi y}}}{\max\left(\frac{e^{-x/2}}{\sqrt{2\pi x}}, \frac{e^{-y/2}}{\sqrt{2\pi y}}\right)} \\
&\quad - 2\min\left(\frac{e^{-x/2}}{\sqrt{2\pi x}}, \frac{e^{-y/2}}{\sqrt{2\pi y}}\right) \qquad \text{[from Lemma B.1]} \\
&\geq 1 - \frac{1}{\min(x,y)} \\
&\quad - \left(\frac{e^{-\max(x,y)/2}}{\max(x,y)\sqrt{\max(x,y)}}\right)\left(\frac{\sqrt{\min(x,y)}}{e^{-\min(x,y)/2}}\right) \\
&\quad - 2\min\left(\frac{e^{-x/2}}{\sqrt{2\pi x}}, \frac{e^{-y/2}}{\sqrt{2\pi y}}\right) \\
&\qquad\qquad \text{[for } x, y > 1\text{]} \\
&\geq 1 - \epsilon. \qquad \text{[for } x, y \text{ sufficiently large]}
\end{aligned}$$

For the upper bound, we have

$$\begin{aligned}
&L_{x,y} \\
&\leq \frac{\left(\frac{e^{-x/2}}{\sqrt{2\pi x}}\right) + \left(\frac{e^{-y/2}}{\sqrt{2\pi y}}\right) - 2\left(1 - \frac{1}{x}\right)\left(\frac{e^{-x/2}}{\sqrt{2\pi x}}\right)\left(1 - \frac{1}{y}\right)\left(\frac{e^{-y/2}}{\sqrt{2\pi y}}\right)}{\max\left(\frac{e^{-2/x}}{\sqrt{2\pi x}}, \frac{e^{-y/2}}{\sqrt{2\pi y}}\right)} \\
&\qquad \text{[from Lemma B.1]} \\
&\leq \frac{\frac{e^{-x/2}}{\sqrt{2\pi x}} + \frac{e^{-y/2}}{\sqrt{2\pi y}}}{\max\left(\frac{e^{-2/x}}{\sqrt{2\pi x}}, \frac{e^{-y/2}}{\sqrt{2\pi y}}\right)} \qquad \text{[for } x, y > 1\text{]} \\
&\leq 2.
\end{aligned}$$

■

*Proof of Theorem IV.2:* As an approximation to $P_e^{(\mathbf{x},i,\mathrm{Rx})}$ given in (18), define

$$\begin{aligned}
&\hat{P}_e^{(\mathbf{x},i,\mathrm{Rx})} \\
&= \frac{1}{\sqrt{2\pi}} \cdot \max\left(\frac{1}{\sqrt{\mathrm{SNR}^{(\mathbf{x},i)}}}\exp\left\{-\frac{SNR^{(\mathbf{x},i)}}{2}\right\}, \right. \\
&\qquad \left. \frac{1}{\sqrt{\mathrm{SNR}^{(i,\mathrm{Rx})}}}\exp\left\{-\frac{SNR^{(i,\mathrm{Rx})}}{2}\right\}\right). \qquad (27)
\end{aligned}$$

For any relay $\mathbf{y}_i$, let

$$\alpha_i = \frac{P_e^{(\mathbf{x},i,\mathrm{Rx})}}{\hat{P}_e^{(\mathbf{x},i,\mathrm{Rx})}}.$$

Let $\epsilon > 0$. Then, using Lemma B.2, it can be shown that

$$1 - \epsilon \leq \alpha_i \leq 2. \tag{28}$$

We will now show that $\sigma_{i,j}$, given by (21), is a finite intersection of unions of certain sets $\rho_{i,j}^{(k)}$ for $k = 1, \ldots, 4$, where each such set has circular and/or linear boundaries.

For each pair of relays $(\mathbf{y}_i, \mathbf{y}_j)$ with $i \neq j$, define

$$\begin{aligned}
\rho_{i,j}^{(1)} &= \left\{\mathbf{x} \in \mathcal{S} : \mathrm{SNR}^{(\mathbf{x},i)} - 2\ln\alpha_i + \ln\mathrm{SNR}^{(\mathbf{x},i)} > \right. \\
&\qquad \left. \mathrm{SNR}^{(\mathbf{x},j)} - 2\ln\alpha_j + \ln\mathrm{SNR}^{(\mathbf{x},j)}\right\} \\
&= \left\{\mathbf{x} \in \mathcal{S} : \frac{2F_2}{C + \|\mathbf{x} - \mathbf{y}_i\|^2} + \frac{N_0}{E_{\mathrm{Tx}}}\ln\left(\frac{\alpha_j}{\alpha_i}\right) \right. \\
&\qquad + \frac{N_0}{E_{\mathrm{Tx}}}\ln\left(\frac{C + \|\mathbf{x} - \mathbf{y}_j\|^2}{C + \|\mathbf{x} - \mathbf{y}_i\|^2}\right) \\
&\qquad \left. > \frac{2F_2}{C + \|\mathbf{x} - \mathbf{y}_j\|^2}\right\}. \\
&\qquad \text{[from (10), (23)]}
\end{aligned}$$

The set $\mathcal{S}$ is bounded, so, using (28), as $E_{\mathrm{Tx}}/N_0 \to \infty$, $E_i/N_0 \to \infty$, and $E_j/N_0 \to \infty$, we have

$$\rho_{i,j}^{(1)} \to \left\{\mathbf{x} \in \mathcal{S} : \|\mathbf{x} - \mathbf{y}_j\|^2 > \|\mathbf{x} - \mathbf{y}_i\|^2\right\}$$

which has a linear internal boundary.

Also, for each pair of relays $(\mathbf{y}_i, \mathbf{y}_j)$ with $i \neq j$, define

$$\rho_{i,j}^{(2)} = \left\{\mathbf{x} \in \mathcal{S} : \mathrm{SNR}^{(\mathbf{x},i)} - 2\ln\alpha_i + \ln\mathrm{SNR}^{(\mathbf{x},i)}\right.$$

$$
\begin{aligned}
&> \mathrm{SNR}^{(j,\mathrm{Rx})} - 2\ln\alpha_j + \ln \mathrm{SNR}^{(j,\mathrm{Rx})}\Big\} \\
&= \Bigg\{ \mathbf{x} \in \mathcal{S} : \frac{2F_2}{C + \|\mathbf{x}-\mathbf{y}_i\|^2} \\
&\qquad > \frac{2F_2}{C + \|\mathbf{y}_j\|^2} \cdot \frac{E_j/N_0}{E_{\mathrm{Tx}}/N_0} \\
&\qquad\quad + \frac{N_0}{E_{\mathrm{Tx}}} \ln\left( \frac{C + \|\mathbf{x}-\mathbf{y}_i\|^2}{C + \|\mathbf{y}_j\|^2} \cdot \frac{E_j/N_0}{E_{\mathrm{Tx}}/N_0} \right) \\
&\qquad\quad + \frac{N_0}{E_{\mathrm{Tx}}} \ln\left(\frac{\alpha_i}{\alpha_j}\right) \Bigg\}. \qquad \text{[from (10),(23)]}
\end{aligned} \tag{29}
$$

In the cases that follow, we will show that, asymptotically, $\rho_{i,j}^{(2)}$ either contains all of the sensors, none of the sensors, or the subset of sensors in the interior of a circle.

**Case 1:** $(E_j/N_0)/(E_{\mathrm{Tx}}/N_0) \to \infty$.

The set $\mathcal{S}$ is bounded and, by (28), $\ln(\alpha_i/\alpha_j)$ is asymptotically bounded. Therefore, the limit of the right-hand side of the inequality in (29) is infinity. Thus, $\rho_{i,j}^{(2)} \to \emptyset$.

**Case 2:** $(E_j/N_0)/(E_{\mathrm{Tx}}/N_0) \to G_j$ for some $G_j \in (0,\infty)$.

Since $\mathcal{S}$ is bounded and $\ln(\alpha_i/\alpha_j)$ is asymptotically bounded, we have

$$
\rho_{i,j}^{(2)} \to \left\{ \mathbf{x} \in \mathcal{S} : \|\mathbf{x}-\mathbf{y}_i\|^2 < \frac{C + \|\mathbf{y}_j\|^2}{G_j} - C \right\}
$$

which has a circular internal boundary.

**Case 3:** $(E_j/N_0)/(E_{\mathrm{Tx}}/N_0) \to 0$.

Since $\mathcal{S}$ is bounded and $\ln(\alpha_i/\alpha_j)$ is asymptotically bounded, the limit of the right-hand side of the inequality in (29) is 0. Thus, since $F_2 > 0$, we have $\rho_{i,j}^{(2)} \to \mathcal{S}$.

Also, for each pair of relays $(\mathbf{y}_i, \mathbf{y}_j)$ with $i \neq j$, define

$$
\begin{aligned}
\rho_{i,j}^{(3)} = \Big\{ \mathbf{x} \in \mathcal{S} : &\ \mathrm{SNR}^{(i,\mathrm{Rx})} - 2\ln\alpha_i + \ln \mathrm{SNR}^{(i,\mathrm{Rx})} \\
&> \mathrm{SNR}^{(\mathbf{x},j)} - 2\ln\alpha_j + \ln \mathrm{SNR}^{(\mathbf{x},j)} \Big\}.
\end{aligned}
$$

Observing the symmetry between $\rho_{i,j}^{(3)}$ and $\rho_{i,j}^{(2)}$, we have that as $E_{\mathrm{Tx}}/N_0 \to \infty$, $E_i/N_0 \to \infty$, and $E_j/N_0 \to \infty$, the set $\rho_{i,j}^{(3)}$ becomes either empty, all of $\mathcal{S}$, or the exterior of a circle.

Also, for each pair of relays $(\mathbf{y}_i, \mathbf{y}_j)$ with $i \neq j$, define

$$
\begin{aligned}
\rho_{i,j}^{(4)} = \Big\{ \mathbf{x} \in \mathcal{S} : &\ \mathrm{SNR}^{(i,\mathrm{Rx})} - 2\ln\alpha_i + \ln \mathrm{SNR}^{(i,\mathrm{Rx})} \\
&> \mathrm{SNR}^{(j,\mathrm{Rx})} - 2\ln\alpha_j + \ln \mathrm{SNR}^{(j,\mathrm{Rx})} \Big\} \\
= \Bigg\{ \mathbf{x} \in \mathcal{S} : &\ \frac{2E_iF_2}{N_0\left(C + \|\mathbf{y}_i\|^2\right)} - \ln\alpha_i \\
&\qquad + \ln\left( \frac{2E_iF_2}{N_0\left(C + \|\mathbf{y}_i\|^2\right)} \right) \\
&> \frac{2E_jF_2}{N_0\left(C + \|\mathbf{y}_j\|^2\right)} - \ln\alpha_j \\
&\qquad + \ln\left( \frac{2E_jF_2}{N_0\left(C + \|\mathbf{y}_j\|^2\right)} \right) \Bigg\}. \\
&\text{[from (10),(23)]}
\end{aligned}
$$

Using (28), as $E_{\mathrm{Tx}}/N_0 \to \infty$, $E_i/N_0 \to \infty$, and $E_j/N_0 \to \infty$, we have $\rho_{i,j}^{(4)} \to \mathcal{S}$ or $\rho_{i,j}^{(4)} \to \emptyset$.

Then, we have

$$
\begin{aligned}
\sigma_{i,j} &= \left\{ \mathbf{x} \in \mathcal{S} : P_e^{(\mathbf{x},i,\mathrm{Rx})} < P_e^{(\mathbf{x},j,\mathrm{Rx})} \right\} \\
&= \left\{ \mathbf{x} \in \mathcal{S} : \alpha_i \hat{P}_e^{(\mathbf{x},i,\mathrm{Rx})} < \alpha_j \hat{P}_e^{(\mathbf{x},j,\mathrm{Rx})} \right\} \\
&= \Big\{ \mathbf{x} \in \mathcal{S} : \min\Big( \mathrm{SNR}^{(\mathbf{x},i)} - 2\ln\alpha_i + \ln \mathrm{SNR}^{(\mathbf{x},i)}, \\
&\qquad\qquad \mathrm{SNR}^{(i,\mathrm{Rx})} - 2\ln\alpha_i + \ln \mathrm{SNR}^{(i,\mathrm{Rx})} \Big) \\
&\qquad\qquad > \min\Big( \mathrm{SNR}^{(\mathbf{x},j)} - 2\ln\alpha_j + \ln \mathrm{SNR}^{(\mathbf{x},j)}, \\
&\qquad\qquad \mathrm{SNR}^{(j,\mathrm{Rx})} - 2\ln\alpha_j + \ln \mathrm{SNR}^{(j,\mathrm{Rx})} \Big) \Big\} \\
&\qquad \text{[for } E_{\mathrm{Tx}}/N_0, E_i/N_0, E_j/N_0 \text{ sufficiently large]} \\
&\qquad\qquad\qquad\qquad \text{[from (27)]} \\
&= \left(\rho_{i,j}^{(1)} \cup \rho_{i,j}^{(2)}\right) \cap \left(\rho_{i,j}^{(3)} \cup \rho_{i,j}^{(4)}\right).
\end{aligned} \tag{30}
$$

Thus, combining the asymptotic results for $\rho_{i,j}^{(1)}, \rho_{i,j}^{(2)}, \rho_{i,j}^{(3)}$, and $\rho_{i,j}^{(4)}$, as $E_{\mathrm{Tx}}/N_0 \to \infty$, $E_i/N_0 \to \infty$, and $E_j/N_0 \to \infty$, the internal boundary of $\sigma_{i,j}$ consists of circular arcs and line segments. Applying (22) completes the proof. ■

## Appendix C: Proof of Theorem IV.3

**Lemma C.1.** *For* $0 < z < 1$,

$$
\begin{aligned}
&\left(\frac{1}{z\Gamma\left(\frac{3}{2}\right)}\right)\left(1-\sqrt{z}\right)\exp\left\{-\frac{\sqrt{z}\left(1-\sqrt{z}\right)^2}{2-\sqrt{z}}\right\} \le U\left(\frac{3}{2},2,z\right) \\
&\qquad\qquad \le \frac{1}{z\Gamma\left(\frac{3}{2}\right)}.
\end{aligned}
$$

*Proof:* For the upper bound, we have

$$
\begin{aligned}
U\left(\frac{3}{2},2,z\right) &= \frac{1}{\Gamma\left(\frac{3}{2}\right)} \int_0^\infty \sqrt{\frac{t}{1+t}} \cdot e^{-zt} dt \\
&\le \frac{1}{\Gamma\left(\frac{3}{2}\right)} \int_0^\infty e^{-zt} dt \\
&= \frac{1}{z\Gamma\left(\frac{3}{2}\right)}.
\end{aligned}
$$

For the lower bound, we have

$$
\begin{aligned}
&U\left(\frac{3}{2},2,z\right) \\
&\ge \frac{1}{\Gamma\left(\frac{3}{2}\right)} \int_{\frac{(1-\sqrt{z})^2}{\sqrt{z}(2-\sqrt{z})}}^\infty \sqrt{\frac{t}{1+t}} \cdot e^{-zt} dt \qquad \text{[since } 0 < z < 1\text{]} \\
&\ge \frac{1}{\Gamma\left(\frac{3}{2}\right)} \int_{\frac{(1-\sqrt{z})^2}{\sqrt{z}(2-\sqrt{z})}}^\infty (1-\sqrt{z}) e^{-zt} dt \qquad \text{[since } 0 < z < 1\text{]} \\
&= \frac{1}{z\Gamma\left(\frac{3}{2}\right)} \left(1-\sqrt{z}\right) \exp\left\{-\frac{\sqrt{z}(1-\sqrt{z})^2}{2-\sqrt{z}}\right\}.
\end{aligned}
$$

■

*Proof of Theorem IV.3:* As an approximation to $P_e^{(\mathbf{x},i,\mathrm{Rx})}$ given in (15), define

$$
\begin{aligned}
\hat{P}_e^{(\mathbf{x},i,\mathrm{Rx})} = \frac{1}{2} &- \left( \frac{D_i\sqrt{\pi}N_0/E_{\mathrm{Tx}}}{8\sigma\left(\sigma^2 + B_iN_0/E_{\mathrm{Tx}}\right)^{3/2}} \right) \\
&\cdot \left( \frac{2\sigma^2\left(\sigma^2 + B_iN_0/E_{\mathrm{Tx}}\right)}{\Gamma(3/2)\cdot D_iN_0/E_{\mathrm{Tx}}} \right)
\end{aligned} \tag{31}
$$

$$= \frac{1}{2} - \frac{1}{2}\left(1 + \frac{1}{2\sigma^2 L_{\mathbf{x},i} E_{\mathrm{Tx}}/N_0}\right)^{-1/2}. \quad \text{[from (14)]} \tag{32}$$

For any relay $\mathbf{y}_i$, let $\alpha_i = \dfrac{P_e^{(\mathbf{x},i,\mathrm{Rx})}}{\hat{P}_e^{(\mathbf{x},i,\mathrm{Rx})}}$. Using Lemma C.1, it can be shown that

$$\lim_{E_{\mathrm{Tx}}/N_0 \to \infty} \alpha_i = 1. \tag{33}$$

Let

$$Z_k = \frac{1}{2\sigma^2 L_{\mathbf{x},k}}$$

$$g_k\left(\frac{N_0}{E_{\mathrm{Tx}}}\right) = \sqrt{1 + \frac{Z_k N_0}{E_{\mathrm{Tx}}}} - 1 = \left(\frac{Z_k}{2}\right)\frac{N_0}{E_{\mathrm{Tx}}} + \mathcal{O}\left(\left(\frac{N_0}{E_{\mathrm{Tx}}}\right)^2\right) \tag{34}$$

where the second equality in the expression for $g_k$ is obtained using a Taylor series. Then,

$$\begin{aligned}
&\sigma_{i,j} \\
&= \left\{\mathbf{x} \in \mathcal{S} : P_e^{(\mathbf{x},i,\mathrm{Rx})} < P_e^{(\mathbf{x},j,\mathrm{Rx})}\right\} \\
&= \left\{\mathbf{x} \in \mathcal{S} : \alpha_i \hat{P}_e^{(\mathbf{x},i,\mathrm{Rx})} < \alpha_j \hat{P}_e^{(\mathbf{x},j,\mathrm{Rx})}\right\} \\
&= \left\{\mathbf{x} \in \mathcal{S} : \frac{\alpha_i\left(\sqrt{1+\frac{Z_i N_0}{E_{\mathrm{Tx}}}} - 1\right)\sqrt{1+\frac{Z_j N_0}{E_{\mathrm{Tx}}}}}{\alpha_j\left(\sqrt{1+\frac{Z_j N_0}{E_{\mathrm{Tx}}}} - 1\right)\sqrt{1+\frac{Z_i N_0}{E_{\mathrm{Tx}}}}} < 1\right\} \quad \text{[from (32), (34)]} \\
&= \left\{\mathbf{x} \in \mathcal{S} : \frac{\alpha_i}{\alpha_j} \cdot \frac{\frac{1}{4\sigma^2 L_{\mathbf{x},i}} + \mathcal{O}\left(\frac{N_0}{E_{\mathrm{Tx}}}\right)}{\frac{1}{4\sigma^2 L_{\mathbf{x},j}} + \mathcal{O}\left(\frac{N_0}{E_{\mathrm{Tx}}}\right)} \cdot \sqrt{\frac{1 + \frac{N_0/E_{\mathrm{Tx}}}{2\sigma^2 L_{\mathbf{x},j}}}{1 + \frac{N_0/E_{\mathrm{Tx}}}{2\sigma^2 L_{\mathbf{x},i}}}} < 1\right\}. \quad \text{[from (34)]}
\end{aligned} \tag{35}$$

Since $\mathcal{S}$ is bounded, we have, for $E_{\mathrm{Tx}}/N_0 \to \infty$, that

$$\sigma_{i,j} \to \{\mathbf{x} \in \mathcal{S} : \|\mathbf{x} - \mathbf{y}_j\| > \|\mathbf{x} - \mathbf{y}_i\|\}. \quad \text{[from (35),(33),(23)]} \tag{36}$$

Thus, for $E_{\mathrm{Tx}}/N_0 \to \infty$, the internal boundary of $\sigma_{i,j}$ becomes the line equidistant from $\mathbf{y}_i$ and $\mathbf{y}_j$. Applying (22) completes the proof. ∎

## APPENDIX D: PROOF OF THEOREM IV.4

**Lemma D.1.** *Let*

$$L_{x,y} = \frac{1 - \left(1 + \frac{2}{x}\right)^{-1/2}\left(1 + \frac{2}{y}\right)^{-1/2}}{\frac{1}{x} + \frac{1}{y}}.$$

*Then,* $\lim_{x,y \to \infty} L_{x,y} = 1$.

*Proof:* We have

$$1 + \frac{1}{2}\epsilon - \frac{1}{8}\epsilon^2 \le (1+\epsilon)^{1/2} \le 1 + \frac{1}{2}\epsilon \quad \text{[from a Taylor series]}$$

$$\therefore \left(\frac{xy}{x+y}\right)\frac{\left(x-\frac{1}{2}\right)\left(y^2+y-\frac{1}{2}\right) + x^2\left(y-\frac{1}{2}\right)}{\left(x^2+x-\frac{1}{2}\right)\left(y^2+y-\frac{1}{2}\right)}$$

$$\le L_{x,y} \le \left(\frac{x+y+1}{x+y}\right)\left(\frac{x}{x+1}\right)\left(\frac{y}{y+1}\right)$$

$$\therefore \left(\frac{x-1}{x+1}\right)\left(\frac{y-1}{y+1}\right)\left(\frac{x+y+3}{x+y}\right)$$

$$\le L_{x,y} \le \left(\frac{x+y+1}{x+y}\right)\left(\frac{x}{x+1}\right)\left(\frac{y}{y+1}\right). \quad \text{[for } x, y \text{ sufficiently large]}$$

Now taking the limit as $x \to \infty$ and $y \to \infty$ (in any manner) gives $L_{x,y} \to 1$. ∎

*Proof of Theorem IV.4:* As an approximation to $P_e^{(\mathbf{x},i,\mathrm{Rx})}$ given in (19), define

$$\hat{P}_e^{(\mathbf{x},i,\mathrm{Rx})} = \frac{1/2}{\mathrm{SNR}^{(\mathbf{x},i)}} + \frac{1/2}{\mathrm{SNR}^{(i,\mathrm{Rx})}}. \tag{37}$$

For any relay $\mathbf{y}_i$, let

$$\alpha_i = \frac{P_e^{(\mathbf{x},i,\mathrm{Rx})}}{\hat{P}_e^{(\mathbf{x},i,\mathrm{Rx})}}.$$

Using Lemma D.1, it can be shown that

$$\lim_{\substack{E_{\mathrm{Tx}}/N_0 \to \infty, \\ E_i/N_0 \to \infty}} \alpha_i = 1. \tag{38}$$

Let $\langle\ ,\ \rangle$ denote the inner product operator. Then, we have

$$\begin{aligned}
\sigma_{i,j} &= \left\{\mathbf{x} \in \mathcal{S} : P_e^{(\mathbf{x},i,\mathrm{Rx})} < P_e^{(\mathbf{x},j,\mathrm{Rx})}\right\} \\
&= \left\{\mathbf{x} \in \mathcal{S} : \alpha_i \hat{P}_e^{(\mathbf{x},i,\mathrm{Rx})} < \alpha_j \hat{P}_e^{(\mathbf{x},j,\mathrm{Rx})}\right\} \\
&= \Bigg\{\mathbf{x} \in \mathcal{S} : 2\langle \mathbf{x}, \alpha_j\mathbf{y}_j - \alpha_i\mathbf{y}_i\rangle \\
&\qquad < \alpha_j\left(C + \|\mathbf{y}_j\|^2\right)\cdot\frac{E_{\mathrm{Tx}}/N_0}{E_j/N_0} \\
&\qquad -\alpha_i\left(C + \|\mathbf{y}_i\|^2\right)\cdot\frac{E_{\mathrm{Tx}}/N_0}{E_i/N_0} \\
&\qquad + (\alpha_j - \alpha_i)\|\mathbf{x}\|^2 + \alpha_j\|\mathbf{y}_j\|^2 - \alpha_i\|\mathbf{y}_i\|^2\Bigg\}. \quad \text{[from (37),(8),(23)]}
\end{aligned} \tag{39}$$

Now, for any relay $\mathbf{y}_k$, let

$$G_k = \lim_{\substack{E_{\mathrm{Tx}}/N_0 \to \infty, \\ E_k/N_0 \to \infty}} \frac{E_k/N_0}{E_{\mathrm{Tx}}/N_0}.$$

Using (38), Table II considers the cases of $G_i$ and $G_j$ being zero, infinite, or finite non-zero; for all such possibilities, the internal boundary of $\sigma_{i,j}$ is linear.

Applying (22) completes the proof. ∎

## REFERENCES


[1] M. Abramowitz and I. A. Stegun, *Handbook of Mathematical Functions with Formulas, Graphs, and Mathematical Tables*. Washington, DC: National Bureau of Standards, 1966.

[2] J. Balam and J. D. Gibson, "Adaptive event coverage using high power mobiles over a sensor field," in *Proc. IEEE 60th Veh. Technol. Conf.*, Los Angeles, CA, Sept. 2004, pp. 4611-4615.

[3] D. Chen and J. N. Laneman, "Modulation and demodulation for cooperative diversity in wireless systems," *IEEE Trans. Wireless Commun.*, vol. 5, no. 7, pp. 1785-1794, 2006.

TABLE II
ASYMPTOTIC PROPERTIES OF $\sigma_{i,j}$ FOR DECODE-AND-FORWARD RELAYS AND RAYLEIGH FADING CHANNELS.

| $G_j$ | $G_i$ | $\sigma_{i,j}$ |
|---|---|---|
| non-zero | non-zero | linear internal boundary |
| non-zero | 0 | $\emptyset$ |
| 0 | non-zero | $\mathcal{S}$ |
| 0 | 0 | linear internal boundary or $\emptyset$ or $\mathcal{S}$ |


[4] Y. Chen, Z. Wang, and J. Liang, "Automatic dynamic flocking in mobile actuator sensor networks by central Voronoi tessellations," in *Proc. IEEE Int. Conf. Mechatronics Automation*, Niagara Falls, Canada, July 2005, pp. 1630-1635.

[5] W. Cho and L. Yang, "Energy and location optimization for relay networks with differential modulation," in *25th Army Science Conf.*, Orlando, FL, Nov. 2006.

[6] C. Comaniciu and H. V. Poor, "On the capacity of mobile ad hoc networks with delay constraints," *IEEE Trans. Wireless Commun.*, vol. 5, no. 8, pp. 2061-2071, 2006.

[7] J. Cortés, S. Martínez, T. Karataş, and F. Bullo, "Coverage control for mobile sensing networks," *IEEE Trans. Robot. Autom.*, vol. 20, no. 2, pp. 243-255, 2004.

[8] S. C. Ergen and P. Varaiya, "Optimal placement of relay nodes for energy efficiency in sensor networks," in *Proc. IEEE Int. Conf. Commun. (ICC)*, Istanbul, Turkey, June 2006, pp. 3473-3479.

[9] A. Gersho and R. M. Gray, *Vector Quantization and Signal Compression*. Norwell, MA: Kluwer Academic Publishers, 1992.

[10] M. O. Hasna and M.-S. Alouini, "End-to-end performance of transmission systems with relays over Rayleigh-fading channels," *IEEE Trans. Wireless Commun.*, vol. 2, no. 6, pp. 1126-1131, 2003.

[11] Y. T. Hou, Y. Shi, H. D. Sherali, and S. F. Midkiff, "On energy provisioning and relay node placement for wireless sensor networks," *IEEE Trans. Wireless Commun.*, vol. 4, no. 5, pp. 2579-2590, 2005.

[12] A. Iranli, M. Maleki, and M. Pedram, "Energy efficient strategies for deployment of a two-level wireless sensor network," in *Proc. Int. Symp. Low Power Electronics Design (ISLPED)*, San Diego, CA, Aug. 2005, pp. 233-238.

[13] I. Koutsopoulos, S. Toumpis, and L. Tassiulas, "On the relation between source and channel coding and sensor network deployment," in *Proc. Int. Workshop Wireless Ad-hoc Networks (IWWAN)*, London, England, May 2005.

[14] X. Liu and P. Mohapatra, "On the deployment of wireless sensor nodes," in *Proc. 3rd Int. Workshop Measurement, Modeling, Performance Analysis Wireless Sensor Networks (SenMetrics)*, San Diego, CA, July 2005, pp. 78-85.

[15] Y. Mao and M. Wi, "Coordinated sensor deployment for improving secure communication and sensing coverage," in *Proc. 3rd ACM Workshop Security Ad Hoc Sensor Networks (SASN)*, Alexandria, VA, Nov. 2005.

[16] L. Ong and M. Motani, "On the capacity of the single source multiple relay single destination mesh network," *Ad Hoc Networks*, vol. 5, no. 6, pp. 786-800, 2007.

[17] J. Pan, L. Cai, Y. T. Hou, Y. Shi, and S. X. Shen, "Optimal base-station locations in two-tiered wireless sensor networks," *IEEE Trans. Mobile Comput.*, vol. 4, no. 5, pp. 458-473, 2005.

[18] J. G. Proakis, *Digital Communications*, 4th edition. New York: McGraw-Hill, 2001.

[19] T. S. Rappaport, *Wireless Communications: Principles and Practice*. Upper Saddle River, NJ: Prentice Hall, 1996.

[20] A. K. Sadek, Z. Han, and K. J. Liu, "An efficient cooperation protocol to extend coverage area in cellular networks," in *Proc. IEEE Wireless Commun. Networking Conf. (WCNC)*, Las Vegas, NV, Apr. 2006, pp. 1687-1692.

[21] A. So and B. Liang, "Exploiting spatial diversity in rate adaptive WLANs with relay infrastructure," in *Proc. IEEE Global Telecommun. Conf. (GLOBECOM)*, St. Louis, MO, Nov. 2005.

[22] J. Suomela, "Approximating relay placement in sensor networks," in *Proc. 3rd ACM Int. Workshop Evaluation Wireless Ad Hoc, Sensor Ubiquitous Networks (PE-WASUN)*, Terromolinos, Spain, Oct. 2006, pp. 145-148.

[23] J. Tan, O. M. Lozano, N. Xi, and W. Sheng, "Multiple vehicle systems for sensor network area coverage," in *Proc. 5th World Conf. Intelligent Control Automation*, Hangzhou, China, June 2004, pp. 4666-4670.

[24] H. L. van Trees, *Detection, Estimation and Modulation Theory, Part 1*. New York: John Wiley & Sons, 1968.

[25] J. M. Wozencraft and I. M. Jacobs, *Principles of Communication Engineering*. New York: John Wiley & Sons, 1965.


**Jillian Cannons** (S'99, M'09) received the B.Sc. degree in computer engineering (with distinction) from the University of Manitoba, Winnipeg, Canada, in 2000; the M.S. degree in electrical engineering from the University of Illinois at Urbana-Champaign, Urbana, IL, in 2002; and the Ph.D. degree in electrical engineering from the University of California, San Diego, in 2008. She is currently a software engineer at Vision Robotics in San Diego.

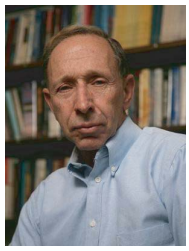

**Laurence B. Milstein** (S'66, M'68, SM'77, F'85) received the B.E.E. degree from the City College of New York, New York, NY, in 1964, and the M.S. and Ph.D. degrees in electrical engineering from the Polytechnic Institute of Brooklyn, Brooklyn, NY, in 1966 and 1968, respectively.

From 1968 to 1974, he was with the Space and Communications Group of Hughes Aircraft Company, and from 1974 to 1976, he was a member of the Department of Electrical and Systems Engineering, Rensselaer Polytechnic Institute, Troy, NY. Since 1976, he has been with the Department of Electrical and Computer Engineering, University of California at San Diego, La Jolla, where he is the Ericsson Professor of Wireless Communications Access Techniques and former Department Chairman, working in the area of digital communication theory with special emphasis on spread-spectrum communication systems. He has also been a consultant to both government and industry in the areas of radar and communications.

Dr. Milstein was an Associate Editor for Communication Theory for the IEEE TRANSACTIONS ON COMMUNICATIONS, an Associate Editor for Book Reviews for the IEEE TRANSACTIONS ON INFORMATION THEORY, an Associate Technical Editor for the IEEE COMMUNICATIONS MAGAZINE, and the Editor-in-Chief of the IEEE JOURNAL ON SELECTED AREAS IN COMMUNICATIONS. He was the Vice President for Technical Affairs in 1990 and 1991 of the IEEE Communications Society, and is a former Chair of the IEEE Fellows Selection Committee. He is a recipient of the 1998 Military Communications Conference Long Term Technical Achievement Award, an Academic Senate 1999 UCSD Distinguished Teaching Award, an IEEE Third Millennium Medal in 2000, the 2000 IEEE Communication Society Armstrong Technical Achievement Award, and various prize paper awards, including the 2002 MILCOM Fred Ellersick Award.

**Kenneth Zeger** (S'85,M'90,SM'95,F'00) was born in Boston in 1963. He received both the S.B. and S.M. degrees in electrical engineering and computer science from the Massachusetts Institute of Technology in 1984, and both the M.A. degree in mathematics and the Ph.D. in electrical engineering at the University of California, Santa Barbara, in 1989 and 1990, respectively. He was an Assistant Professor of Electrical Engineering at the University of Hawaii from 1990 to 1992. He was in the Department of Electrical and Computer Engineering and the Coordinated Science Laboratory at the University of Illinois at Urbana-Champaign, as an Assistant Professor from 1992 to 1995, and as an Associate Professor from 1995 to 1996. He has been in the Department of Electrical and Computer Engineering at the University of California at San Diego, as an Associate Professor from 1996 to 1998, and as a Professor from 1998 to present. He received an NSF Presidential Young Investigator Award in 1991. He served as Associate Editor At-Large for the IEEE TRANSACTIONS ON INFORMATION THEORY during 1995-1998, as a member of the Board of Governors of the IEEE Information Theory Society during 1998-2000, 2005-2007, and 2008-2010, and is an IEEE Fellow.